Politecnico di Torino

Porto Institutional Repository

[Proceeding] Optimal Inverse Method for Turbomachinery Design

(Article begins on next page)
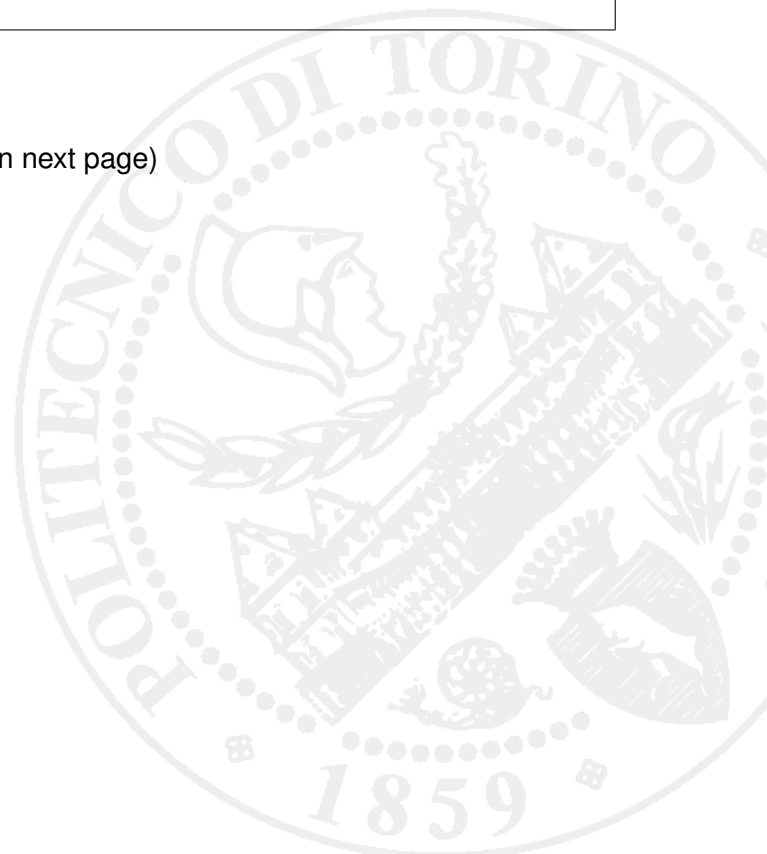
OPTIMAL INVERSE METHOD FOR TURBOMACHINERY DESIGN

M. Ferlauto, A. Iollo and L. Zannetti

Dipartimento di Ingegneria Aeronautica e Spaziale
Politecnico di Torino, c.so Duca degli Abruzzi, 24, 10129 Torino, Italy
Email: ferlauto@athena.polito.it, iollo@aethon.polito.it, zannetti@polito.it

Key words: Optimization, Inverse Design, Turbomachinery Flows

Abstract. *An adjoint optimization method based on the solution of an inverse problem is proposed. In this formulation, the distributed control is a flow variable on the domain boundary, for example pressure. The adjoint formulation delivers the functional gradient with respect to such flow variable distribution, and a descent method can be used for optimization. The flow constraints are easily imposed in the parametrization of the controls, thus those problems with many strict constraints on the flow solution can be solved very efficiently. Conversely, the geometric constraints are imposed either by additional partial differential equations, or by penalization. Constraining the geometric solution, the classical limitations of the inverse problem design are overcome. Two examples pertaining to internal flows are given.*

1

1 INTRODUCTION

Usual optimization methods iterate on the geometry of a certain flow problem to determine a configuration minimizing or maximizing a given objective function, i.e., for each optimization step a direct problem is solved [1]. In the present study we propose to iterate on inverse problems [2][3], motivated by the fact that in such formulation fluid-dynamic constraints on the solution are very easily imposed. In the following, the optimization procedure is explained through its application to two problems of interest in the turbomachinery design practice. The first case concerns the problem of designing a diffuser for maximal axial component of the flow at the outlet, with a maximum allowed pressure gradient at the wall.

In the second example we investigate the application of the adjoint optimization method to the flow design of turbomachinery bladings, based on a simplified model. The blades of the turbomachine are modeled as flow surfaces of zero thickness which exert forces on the fluid flow. This approximation introduces volume forces in the compressible Euler equations, which is the model adopted for the flow. In our approach, instead of modifying the shape of the flow surfaces modeling the blades, we give the force which the blades exert on the flow, and let the geometry accommodate such distribution of forces. Then the volume force distribution itself varies based on the functional gradient, so that, for example, thrust is maximized.

2 DIFFUSER WITH MINIMAL AXIAL DEVIATION AT THE OUTLET

We consider a two-dimensional diffuser where the total pressure, total temperature and flow incidence are imposed at inlet and the static pressure is given at outlet. The aim is to design the diffuser walls so that the flow has minimal axial deviation at outlet, satisfying some requirements on the wall pressure gradient to avoid premature flow detachments. This simple problem finds its applications in the design of wind tunnels diffusers, air intakes of airbreathing engines, or turbomachines casing.

2.1 Flow model and inverse problem

The flow considered is governed by the two-dimensional compressible Euler equations. In a cartesian frame of reference, we have

$$\frac{\partial \boldsymbol{U}}{\partial t} + \frac{\partial \boldsymbol{F}}{\partial x} + \frac{\partial \boldsymbol{G}}{\partial r} = 0 \tag{1}$$

and

$$\boldsymbol{U} = \left\{ \begin{array}{c} \rho \\ \rho u \\ \rho w \\ e \end{array} \right\}, \quad \boldsymbol{F} = \left\{ \begin{array}{c} \rho u \\ p + \rho u^2 \\ \rho u w \\ u(p + e) \end{array} \right\} \quad \boldsymbol{G} = \left\{ \begin{array}{c} \rho w \\ \rho u w \\ p + \rho w^2 \\ w(p + e) \end{array} \right\} \tag{2}$$

2

as usual ρ is density, p pressure, e total internal energy per unit volume.

The solution of the inverse problem is based on the ideas presented in [2] and [3]. The diffuser wall to be designed, can be seen as a deformable and impermeable surface constrained to the diffuser inlet section. It moves under the effect of the external pressure imposed on its walls. An initial configuration of such surfaces is guessed. The following transient is described by integrating in time the equations governing the time dependent flow motion using a finite volume formulation, based on an approximate Riemann solver [4] to compute the fluxes at cell interfaces. Second order spatial accuracy is obtained by an ENO class method [5]. At the end of the transient, the walls assume the shape that solve the inverse problem, i.e., find the shape which realize the given pressure distribution on the walls.

2.2 Variational formulation, adjoint equations and gradient

We want to determine the wall pressure $p_\gamma(s)$, so that the functional

$$D[p_\gamma(s)] = \frac{1}{2} \int_{out} \left(\frac{w}{u} \right) \, dz \tag{3}$$

is minimum subject to the flow equations. In order to solve such constrained minimization problem we introduce the Lagrangian function

$$\mathcal{L}(\boldsymbol{U}, p_\gamma, \boldsymbol{\Lambda}) = D + \int_\Omega {}^t\boldsymbol{\Lambda} \; \boldsymbol{E}(\boldsymbol{U}, p_\gamma) \, d\Omega \tag{4}$$

where ${}^t\boldsymbol{\Lambda}(x, r) = (\lambda_1, \lambda_2, \lambda_3, \lambda_4)$ are Lagrange multipliers. The Lagrangian will allow us to treat the minimization problem as an unconstrained problem. A stationary point is found when the variation of $\mathcal{L}$ vanishes with respect to all of its arguments, which are now considered independent functions. We compute $\delta\mathcal{L}$ as in [1].

We have

$$\delta\mathcal{L} = \delta\mathcal{L}_U + \delta\mathcal{L}_{p_\gamma} + \delta\mathcal{L}_\Lambda \tag{5}$$

with

$$\delta\mathcal{L}_U = \delta D_U + \int_\Sigma {}^t\boldsymbol{\Lambda}(\boldsymbol{F}_U \, n_x + \boldsymbol{G}_U \, n_z)\delta\boldsymbol{U} \, d\sigma - \int_\Omega ({}^t\boldsymbol{\Lambda}_x \, \boldsymbol{F}_U + {}^t\boldsymbol{\Lambda}_z \, \boldsymbol{G}_U)\delta\boldsymbol{U} \, d\Omega \tag{6}$$

where Σ is the entire border of the flow field Ω, and $\boldsymbol{F}_U$, $\boldsymbol{G}_U$ are the Jacobian matrices. In order to have $\delta\mathcal{L} = 0$, all the single contributions to $\delta\mathcal{L}$ must vanish at the minimum. Therefore, to find a stationary point, we enforce

$$\delta\mathcal{L}_U = 0, \qquad \delta\mathcal{L}_\Lambda = 0 \tag{7}$$

In general this results in $\delta\mathcal{L}_{p_\gamma} \neq 0$. To reach the minimum we take δp_γ such that $\delta\mathcal{L}_{p_\gamma} < 0$, for example using a conjugate gradient method. Note that the variations of $\delta\mathcal{L}$ with respect to the Lagrange multipliers $\boldsymbol{\Lambda}$ simply yield the flow equations.

From the condition $\delta\mathcal{L}_U = 0$ we obtain the so called "adjoint" of the Euler equations and its boundary conditions, that is

$$^t\mathbf{\Lambda}_x\,\mathbf{F}_U + {}^t\mathbf{\Lambda}_z\,\mathbf{G}_U = 0 \qquad in\ \Omega \tag{8}$$

and

$$\left[\frac{w}{u}\frac{\partial}{\partial\mathbf{U}}\left(\frac{w}{u}\right)h(\Sigma) + {}^t\mathbf{\Lambda}(\mathbf{F}_U\,n_x + \mathbf{G}_U\,n_z)\right]\delta\mathbf{U} = 0 \qquad on\ \Sigma \tag{9}$$

where $h(\Sigma)$ is 1 at the outlet and 0 elsewhere. From the above equation we derive the boundary condition for the adjoint.

For given pressure at the wall, the adjoint boundary condition is

$$\lambda_1 + u\lambda_2 + w\lambda_3 + (e + \frac{p}{\rho})\lambda_4 = 0 \tag{10}$$

The functional gradient is

$$\delta D_{p_\gamma} = \int_{wall}(\lambda_2 n_x + \lambda_3 n_z)\delta p\,ds \tag{11}$$

The wall pressure distribution must be constrained in order to obtain meaningful solutions. Indeed, if the pressure is let free to vary, a constant pressure distribution would represent an admissible solution, leading to a diffuser with parallel walls. Therefore we consider a diffuser, with imposed inlet p_{in} and outlet p_{out} pressures. The main design limitation is the maximum pressure gradient allowed in order to avoid detachment. Assuming as control the pressure gradient at wall, we recover the pressure as

$$p_\gamma(x_k) = p_{in} + \sum_{j=2}^{k} m(x_j)dxj, \qquad m(x_j) = \left(\frac{dp_\gamma}{dx}\right)_j \tag{12}$$

with the constraint

$$\sum_{j=2}^{N} m(x_j)dx_j = p_{out} - p_{in} \tag{13}$$

to match the exit pressure. N is the number of computational points in the x-direction.

The solution of the optimization problem is achieved by initializing the coefficients $m(x_j)$, computing the corresponding wall geometry by the inverse problem, solving the adjoint equations and updating the coefficients $m(x_j)$ according to the gradient eq.(11) until the minimum is reached.

3   FAN STAGE WITH MAXIMUM THRUST

The fan of a turbojet engine is composed by a rotor, which works on the flow, and a stator to deflect the flux. We want to determine by a simplified flow model, the rotor and stator geometries resulting in maximum thrust of the fan. The work done on the fluid is kept constant.

3.1 Turbomachine flow model in the meridional plane

The flow deflection through rotors and stators of a turbomachine is the result of the forces that rotors and stators blades exert on the flow. An axial-symmetric model of a turbomachine can be set up by replacing the blade rows with volume forces. We assume that the blade rows have vanishing thickness and infinite solidity, so that the single blade coincides with a stream surface. Thus, in the case of an inviscid flow, the effect of solid blades is modeled by volume forces orthogonal to stream surfaces.
Let

$$\boldsymbol{F} = F^x\,\boldsymbol{i} + F^r\,\boldsymbol{\xi} + F^\vartheta\,\boldsymbol{\eta} \tag{14}$$

be the volume force, where $\boldsymbol{i}$, $\boldsymbol{\xi}$ and $\boldsymbol{\eta}$ are the unit vectors pertinent to the axial, radial and tangential directions in a cylindrical frame of reference $\{x\,\boldsymbol{i},\,r\,\boldsymbol{\xi},\,\vartheta\,\boldsymbol{\eta}\}$.
The distribution of the tangential component $F^\vartheta = F^\vartheta(x,r,\vartheta)$ is the function to be optimized, the same way the shape of a wall is typically optimized in usual optimization algorithms.
The geometry of the blades, represented by 2D manifolds

$$\Theta(x,r,\vartheta) = 0. \tag{15}$$

is found by solving

$$(\boldsymbol{q} - j\omega r\eta) \cdot \nabla\Theta = 0, \tag{16}$$

as the blades are to be stream surfaces of the absolute or relative motion for stators and rotors respectively. In the equation above $\boldsymbol{q} = u\,\boldsymbol{i} + w\,\boldsymbol{\xi} + v\,\boldsymbol{\eta}$ is the flow velocity vector, ω is the angular velocity of rotors and $j = 0$ for stators, $j = 1$ for rotors.
The components of the volume force F^x and F^r are determined enforcing the blade manifolds to be orthogonal to the volume forces

$$\boldsymbol{F} \times \nabla\Theta = 0. \tag{17}$$

which implies

$$F^x = r\frac{\Theta_x}{\Theta_\vartheta}F^\vartheta, \qquad F^r = r\frac{\Theta_r}{\Theta_\vartheta}F^\vartheta \tag{18}$$

3.2 Inverse problem

In this section we detail the solution technique of the inverse problem taking as known $F^\vartheta(x,r,\vartheta)$. However, it should be noted that this distribution is updated during the optimization in order to maximize a cost function which in our case is thrust.
The solution of the inverse design problem is obtained by means of a time dependent process. The blades can be seen as deformable and impermeable surfaces constrained to the leading edge, like fastened sails waving under the wind effect. An initial configuration of such surface is guessed. The following transient is described by integrating in time the equations governing the time dependent flow motion. At the end of the transient the

blades assume the shape that solve the inverse problem.

In a cylindrical frame of reference, the compressible Euler equations with volume forces acting on the fluid are

$$\frac{\partial \boldsymbol{U}}{\partial t} + \frac{\partial \boldsymbol{A}}{\partial x} + \frac{\partial \boldsymbol{B}}{\partial r} + \boldsymbol{Q} = 0 \tag{19}$$

where

$$\boldsymbol{U} = \left\{ \begin{array}{c} \rho \\ \rho u \\ \rho v \\ \rho w \\ e \end{array} \right\}, \quad \boldsymbol{A} = \left\{ \begin{array}{c} \rho u \\ p + \rho u^2 \\ \rho u v \\ \rho u w \\ u(p + e) \end{array} \right\} \quad \boldsymbol{B} = \left\{ \begin{array}{c} \rho w \\ \rho u w \\ \rho v w \\ p + \rho w^2 \\ w(p + e) \end{array} \right\} \tag{20}$$

$$\boldsymbol{Q} = \left\{ \begin{array}{c} \dfrac{\rho w}{r} + \rho u \alpha \\[2mm] \dfrac{\rho u w}{r} - F^x + \rho u^2 \alpha \\[2mm] 2\dfrac{\rho v w}{r} - F^\theta \\[2mm] \dfrac{\rho(v^2 - w^2)}{r} - F^r \\[2mm] \dfrac{w(p + e)}{r} - \boldsymbol{F} \cdot \boldsymbol{q} + u(p + e)\alpha \end{array} \right\}$$

as usual ρ is density, p pressure, e total internal energy per unit volume.

The boundary condition at the entry section are the two ratios between the velocity components, the total pressure and the total temperature when the flow is subsonic, while all the flow properties are prescribed if the flow is supersonic; at the exit section the static pressure is prescribed if the flow is subsonic, while no boundary conditions are needed when the flow is supersonic. The blades blockage is taken into account by the terms containing the coefficient α, with

$$\alpha = \frac{\partial}{\partial x}[\log(2\pi r - T)] \tag{21}$$

where $T = T(x, r)$ is the sum of the estimated blades thickness, including the boundary layers.

The system of eqs.19 is integrated in time using a finite volume formulation based on an approximate Riemann solver [4] to compute the fluxes at cell interfaces. Second order spatial accuracy is obtained by an ENO class method [5].

A blade surface changes its shape during the transient to obey the condition of impermeability. Let us express eq.15 as

$$\Theta(x, r, \vartheta, t) = \vartheta - g(x, r, t) = 0 \tag{22}$$

so that eqs. 18 become

$$F^x = -rg_x F^\vartheta, \qquad F^r = -rg_r F^\vartheta \qquad (23)$$

Flow particles on $\Theta(x, r, \vartheta, t) = 0$ must remain on the manifold for the impermeability condition. It follows that during the transient the Langragian derivative of the function $\Theta(x, r, \vartheta, t)$ has to be null

$$\frac{d\Theta}{dt} = \Theta_t + (q - j\omega r\eta) \cdot \nabla\Theta = 0 \qquad (24)$$

that can be written as

$$g_t = -ug_x - wg_r + \frac{v - j\omega r}{r} \qquad (25)$$

with $j = 0$ for stators and $j = 1$ for rotors. The above equation is solved coupled to the Euler equations, and it is integrated in time upwinding the spatial derivatives of g according to u and w.

3.3 Flow equations adjoint

In this section we derive the functional differential using the adjoint technique. As a functional we consider the conventional thrust expressed as

$$T = \left[\int_{r_h}^{r_t} (p + \rho u^2) r \, dr\right]_{outlet} - \left[\int_{r_h}^{r_t} (p + \rho u^2) r \, dr\right]_{inlet} = \int_{\Gamma_{io}} H(U) \, d\Gamma \qquad (26)$$

where F^ϑ, the distribution of tangential forces, is the control, r_t and r_h are the tip and hub radius respectively. The maximum of T is constrained by the steady state Euler equations

$$\boldsymbol{E}(F^\vartheta) = \boldsymbol{A}_x + \boldsymbol{B}_r + \boldsymbol{Q} = 0 \qquad (27)$$

and by the kinematic constraint on the blades

$$\boldsymbol{G}(\boldsymbol{U}(F^\vartheta)) = ug_x + wg_r - \frac{v - j\omega r}{r} = 0 \qquad (28)$$

In order to solve such constrained maximization problem we introduce the Lagrangian function

$$\mathcal{L}(\boldsymbol{U}, g, F^\vartheta, \Lambda, \mu) = \int_{\Gamma_{io}} \boldsymbol{H}(\boldsymbol{U}) \, d\Gamma + \int_\Omega {}^t\boldsymbol{\Lambda} \, \boldsymbol{E}(\boldsymbol{U}, F^\vartheta, g) \, d\Omega + \int_\Omega \mu \, G(\boldsymbol{U}, g) \, d\Omega \qquad (29)$$

where ${}^t\boldsymbol{\Lambda}(x, r) = (\lambda_1, \lambda_2, \lambda_3, \lambda_4, \lambda_5)$ and $\mu = \mu(x, r)$ are Lagrange multipliers. A stationary point is found when the variation of $\mathcal{L}$ with respect to all of its arguments, considered as independent functions, is 0. We have

$$\delta\mathcal{L} = \delta\mathcal{L}_U + \delta\mathcal{L}_{F^\vartheta} + \delta\mathcal{L}_g + \delta\mathcal{L}_\Lambda + \delta\mathcal{L}_\mu \qquad (30)$$

In order to have $\delta\mathcal{L} = 0$, all the single contributions to $\delta\mathcal{L}$ must vanish at the maximum, so that we enforce

$$\delta\mathcal{L}_U = 0 \qquad \delta\mathcal{L}_\Lambda = 0 \qquad \delta\mathcal{L}_\mu = 0 \qquad \delta\mathcal{L}_g = 0$$

In general this results in $\delta\mathcal{L}_{F^\vartheta} \neq 0$. To reach the maximum we take δF^ϑ such that $\delta\mathcal{L} = \delta\mathcal{L}_{F^\vartheta} > 0$, for example using a conjugate gradient method, as explained in the following.

From the condition $\delta\mathcal{L}_U = 0$ we obtain the so called *adjoint* of the Euler equations and its boundary conditions, that is

$$^t\mathbf{\Lambda}_x \, \mathbf{A}_U + {}^t\mathbf{\Lambda}_r \, \mathbf{B}_U - {}^t\mathbf{\Lambda} \, \frac{\partial \mathbf{Q}}{\partial \mathbf{U}} - \mu \frac{\partial G}{\partial \mathbf{U}} = 0 \ \ on \ \Omega \tag{31}$$

and

$$\left[\frac{\partial \mathbf{H}^*}{\partial \mathbf{U}} + {}^t\mathbf{\Lambda} \left(\mathbf{A}_U \, n_x + \mathbf{B}_U \, n_r \right) \right] \delta \mathbf{U} = 0 \qquad on \ \Sigma \tag{32}$$

where $H^* = H$ for the inlet and the outlet, and $H^* = 0$ elsewhere.

The condition $\delta\mathcal{L}_g = 0$ yields to the adjoint of the kinematic constraint as

$$(\mu u)_x + (\mu u)_r + \nabla \cdot ({}^t\mathbf{\Lambda} \, \mathbf{K}) = 0 \qquad in \ \Omega_b \tag{33}$$

where $\mathbf{n} = (n_x, n_y)$ and

$$\mathbf{K} = r F^\vartheta \left\{ \begin{array}{cc} 0 & 0 \\ 1 & 0 \\ 0 & 0 \\ 0 & 1 \\ u & w \end{array} \right\}$$

together with the boundary condition

$$\left[\mu \left(\mathbf{q} \cdot \mathbf{n} \right) + ({}^t\mathbf{\Lambda} \, \mathbf{K}) \cdot \mathbf{n} \right] \delta g = 0 \qquad on \ \Gamma_b \tag{34}$$

The adjoint equation of the kinematic constraint is coupled to eq. (31) the same way the kinematic constraint is coupled to the flow equations.

Note that the variations of $\mathcal{L}$ with respect to the Lagrange multipliers Λ and μ simply yield the flow equations and the kinematic constraint respectively.

Finally, we are left with

$$\delta\mathcal{L} = \delta\mathcal{L}_{F^\vartheta} = \int_{\Omega_b} {}^t\mathbf{\Lambda} \, \frac{\partial \mathbf{Q}}{\partial F^\vartheta} \delta F^\vartheta \, d\Omega \tag{35}$$

This functional depends on $\mathbf{U}$, $\mathbf{\Lambda}$, μ; variables that satisfy the flow equations, the kinematic constraint and the respective adjoints. Therefore if we update the present distribution of F^ϑ with

$$\delta F^\vartheta = \varrho \, {}^t\mathbf{\Lambda} \, \frac{\partial \mathbf{Q}}{\partial F^\vartheta} \tag{36}$$

taking $\varrho > 0$, then $\delta\mathcal{L} > 0$. Iterating such procedure the maximum is eventually reached.

This method, namely the gradient method, has a very slow convergence rate. Better convergence rates are obtained with the conjugate gradient method [6], in which the correction to F^ϑ at the iterate k is

$$(\delta F^\vartheta)^k = \varrho \left[\psi^k - \beta^{k-1}(\delta F^\vartheta)^{k-1}\right] \tag{37}$$

with

$$\beta^{k-1} = \frac{\displaystyle\int_{\Omega_b} [\psi^k - \psi^{k-1}]\,\psi^k d\Omega}{\displaystyle\int_{\Omega_b} [\psi^{k-1}]^2\,d\Omega} \tag{38}$$

where

$$\psi = {}^t\boldsymbol{\Lambda}\,\frac{\partial\boldsymbol{Q}}{\partial F^\vartheta} \tag{39}$$

4   ADJOINT EQUATIONS NUMERICAL SOLUTION

The numerical solution of the adjoint equations is obtained by using a first-order time-dependent technique based on a finite volume discretization. The solver computes the fluxes at cell interfaces by a flux-vector splitting technique. In a similar way, the boundary conditions are imposed on the computational field edges.

Consider the adjoint equations. If a time derivative $-{}^t\boldsymbol{\Lambda}_\tau$ is added to eqs.(31), (32) we are led to the hyperbolic system

$${}^t\boldsymbol{\Lambda}_\tau - {}^t\boldsymbol{\Lambda}_x\,\boldsymbol{A_U} - {}^t\boldsymbol{\Lambda}_r\,\boldsymbol{B_U} + {}^t\boldsymbol{\Lambda}\,\boldsymbol{Q_U} + \mu\,\boldsymbol{G_U} = 0 \tag{40}$$

with the same boundary condition of (31), that is

$$\left[\frac{\partial\boldsymbol{H}^*}{\partial\boldsymbol{U}} + {}^t\boldsymbol{\Lambda}\,(\boldsymbol{A_U}\,n_x + \boldsymbol{B_U}\,n_r)\right]\delta\boldsymbol{U} = 0 \tag{41}$$

The system (40) is linear, because $\boldsymbol{A_U}$, $\boldsymbol{B_U}$, $\boldsymbol{Q_U}$, $\boldsymbol{G_U}$, depend only on x and r, and its characteristics are the same as those of the flow problem, but with opposite speed. We set

$${}^t\boldsymbol{\Lambda}_x\,\boldsymbol{A_U} = ({}^t\boldsymbol{\Lambda}\,\boldsymbol{A_U})_x - {}^t\boldsymbol{\Lambda}(\boldsymbol{A_U})_x \tag{42}$$

$${}^t\boldsymbol{\Lambda}_r\,\boldsymbol{B_U} = ({}^t\boldsymbol{\Lambda}\,\boldsymbol{B_U})_r - {}^t\boldsymbol{\Lambda}(\boldsymbol{B_U})_r \tag{43}$$

then, substituting in (40), we have

$${}^t\boldsymbol{\Lambda}_\tau - [{}^t\boldsymbol{\Lambda}\,\boldsymbol{A}_U]_x - [{}^t\boldsymbol{\Lambda}\,\boldsymbol{B}_U]_r + {}^t\boldsymbol{\Lambda}[(\boldsymbol{A}_U)_x + (\boldsymbol{B}_U)_r] + {}^t\boldsymbol{\Lambda}\,\boldsymbol{Q_U} + \mu\,\boldsymbol{G_U} = 0 \tag{44}$$

Considering an elementary volume of integration Ω with surface σ, we can write eq. (44) in conservation form and apply the Gauss theorem to obtain

$$\frac{\partial}{\partial\tau}\int_\Omega {}^t\boldsymbol{\Lambda}\,d\Omega - \int_\sigma {}^t\boldsymbol{\Lambda}\,\boldsymbol{C}\,d\sigma + {}^t\boldsymbol{\Lambda}\int_\sigma \boldsymbol{C}\,d\sigma + \int_\Omega ({}^t\boldsymbol{\Lambda}\,\boldsymbol{Q_U} + \mu\,\boldsymbol{G_U})d\Omega = 0 \tag{45}$$

9

with $\boldsymbol{C} = \boldsymbol{A_U}\, n_x + \boldsymbol{B_U}\, n_r$. In the above formula we considered $\boldsymbol{\Lambda}$ piecewise constant over the discretization volume. A characteristic-based approach is used to evaluate the convective fluxes at the cell interfaces. The total flux across the interface (int) is evaluated as sum of two contributions which arise from the left (l) and right (r) side of the interface, according to the wave-propagating nature of the hyperbolic system

$$({}^t\boldsymbol{\Lambda}\,\boldsymbol{C})_{int} = ({}^t\boldsymbol{\Lambda}^+\,\boldsymbol{C}^+)_l + ({}^t\boldsymbol{\Lambda}^-\,\boldsymbol{C}^-)_r \qquad (46)$$

where

$$\boldsymbol{C}^+ = \boldsymbol{L}\,\boldsymbol{D}^+\,\boldsymbol{R}, \qquad\qquad \boldsymbol{C}^- = \boldsymbol{L}\,\boldsymbol{D}^-\,\boldsymbol{R} \qquad (47)$$

and $\boldsymbol{D}^+ + \boldsymbol{D}^- = \boldsymbol{D}$. The matrix D is a diagonal matrix having as track the eigenvalues of $\boldsymbol{C}$, that is

$$\boldsymbol{D}^+ + \boldsymbol{D}^- = \boldsymbol{D} = \begin{pmatrix} V_n & 0 & 0 & 0 & 0 \\ 0 & V_n & 0 & 0 & 0 \\ 0 & 0 & V_n & 0 & 0 \\ 0 & 0 & 0 & V_n - a & 0 \\ 0 & 0 & 0 & 0 & V_n + a \end{pmatrix} \qquad (48)$$

The matrices $\boldsymbol{D}^+$ and $\boldsymbol{D}^-$ are diagonal as well, and they consist of the positive and negative eigenvalues of $\boldsymbol{C}$ respectively. The adjoint equation (33) for the kinematic constraint can be manipulated in a similar way. By adding a time derivative $-\mu_\tau$ we have

$$\mu_\tau - (\mu u)_x - (\mu w)_r + \nabla \cdot ({}^t\boldsymbol{\Lambda}\,\boldsymbol{K}) = 0 \qquad (49)$$

Once again the sign of the time derivate has been chosen in order to obtain a well-posed problem. The finite volume approximation is straightforward

$$\frac{\partial}{\partial \tau} \int_{\Omega_b} \mu\, d\Omega - \int_{\Gamma_b} \mu(u n_x + w n_r)\, d\Gamma + \int_{\Gamma_b} ({}^t\boldsymbol{\Lambda}\,\boldsymbol{K}) \cdot \boldsymbol{n}\, d\Gamma = 0 \qquad (50)$$

where Ω_b is the projection of the blade surface onto meridional plane, and Γ_b its contour.

5   RESULTS

5.1   Diffuser

The diffuser is discretized over a 40×20 grid. The inlet pressure is $p_{in} = 0.83$, the outlet pressure $p_{out} = 0.944$. The imposed flow angle at the inlet varies from zero, at the bottom wall, to 10 degrees, at the upper wall. We are looking for the diffuser geometry that better approximate a zero flow angle at the outlet. As already told, the control is here represented by the pressure gradient at each computational point lying on the upper wall. The number mj of design variables is one less than the grid discretization in the x direction, therefore $mj = 39$.

As initial wall pressure distribution, we enforced a parabolic profile (see figure 3a), which
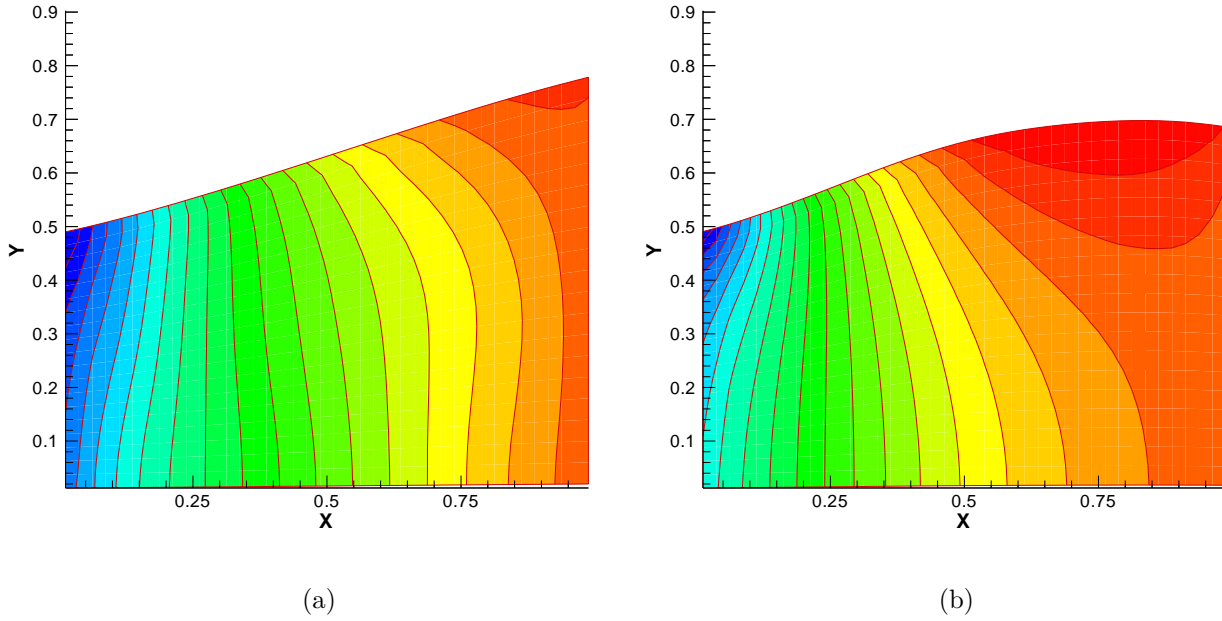
(a)   (b)

Figure 1: Diffuser. Geometry and pressure field before (a) and after (b) the optimization process.

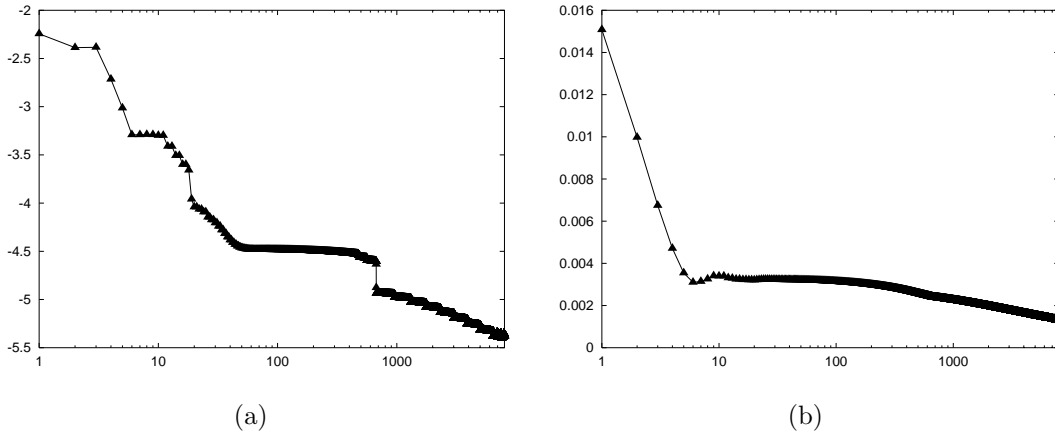(a)   (b)

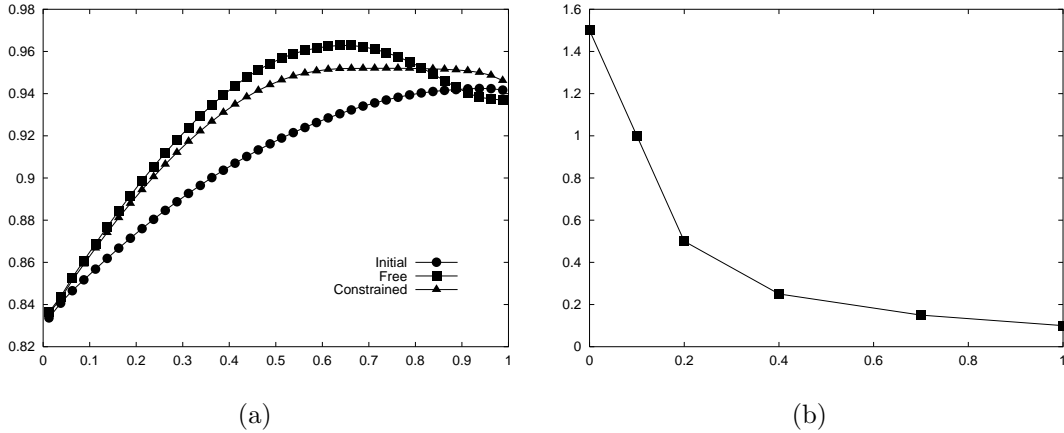Figure 2: Diffuser. Gradient residual and flow alignment versus optimization steps.

11

Figure 3: Diffuser. (a) Optimal pressure distribution on the upper wall, (b) constraint on the pressure gradient along the x-direction.

also satisfies the constraint on the pressure gradient. This constraint is based on mixed theoretical and empirical considerations about the reasonable range of pressure gradients attainable without incurring in flow separations. We represented it schematically as the function $\pi(x)$ shown in fig. (3b).

In figure 1 the initial and the final geometry of the diffuser are depicted. The initial geometry is characterized by a non-zero flow angle σ_{out} at the exit. After the optimization process the condition $\sigma_{out} = 0$ is matched with good approximation (figure 2b). The l^2 norm of the gradient residuals is presented in figure 2a.

5.2 Fan stage

The distributed control F^θ is null everywhere except on the blades, where it is discretized only along the radial direction. We have

$$F^\theta(x, r_i) = \mathcal{F}(r_i) \left[1 - \cos\left(2\pi \frac{x - x_t}{x_l - x_t} \right) \right] \tag{51}$$

so that the load on the leading ($x = x_l$) and trailing ($x = x_t$) edges is 0. For each blade considered we have as many design parameters $\mathcal{F}(r_i)$ as the number of computational points in the radial direction.

Equation (35) is discretized as

$$\delta \mathcal{L} = \sum_i \delta \mathcal{F}(r_i) L(r_i)(r_i - r_{i-1}) \tag{52}$$

where

$$L(r_i) = \sum_j {}^t\mathbf{\Lambda}(x_j, r_i) \frac{\partial \mathbf{Q}}{\partial F^\vartheta}(x_j, r_i) \left[1 - \cos\left(2\pi \frac{x - x_t}{x_l - x_t} \right) \right] (x_j - x_{j-1}) \tag{53}$$
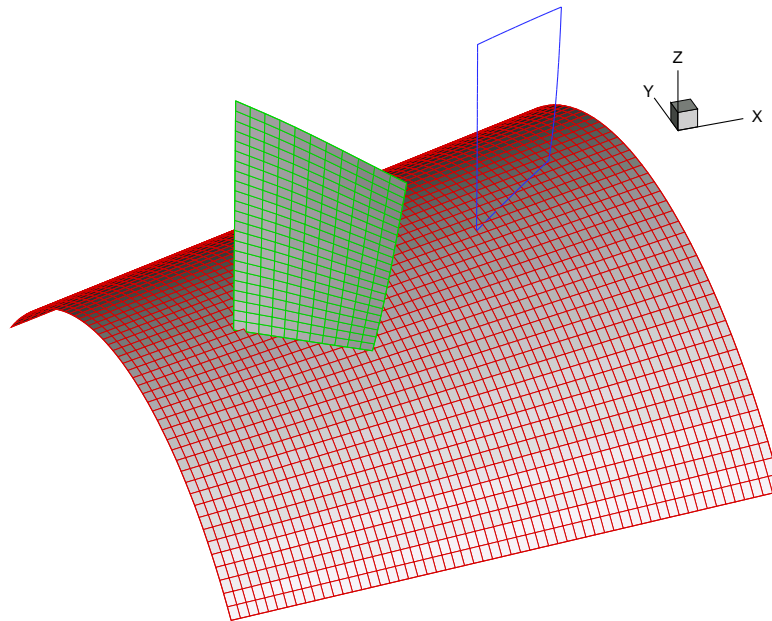
12

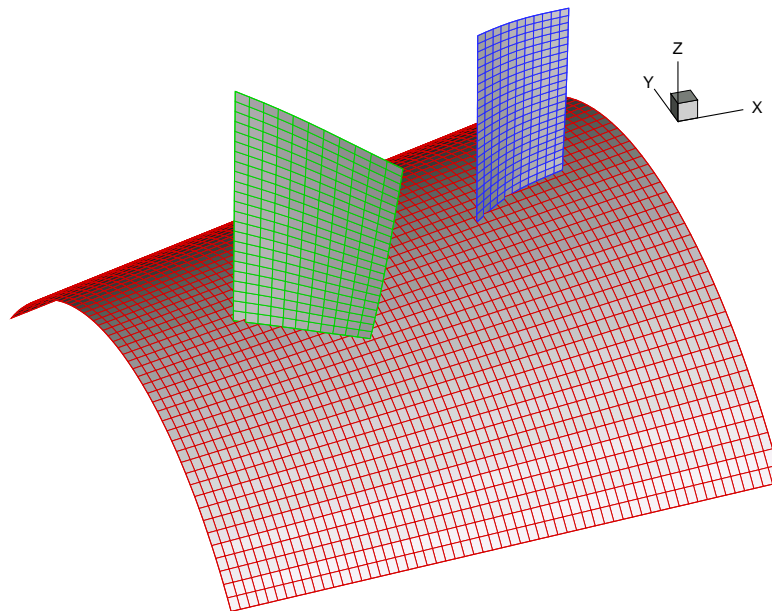Figure 4: Fan stage. Initial geometry .

Figure 5: Fan Stage. Final geometry.

13

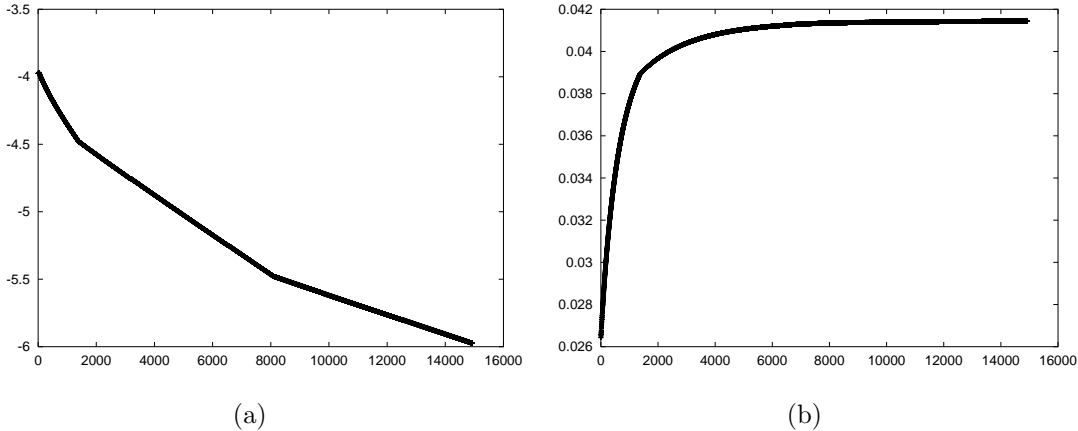(a)   (b)

Figure 6: Fan stage. Gradient residual (a) and thrust (b) versus optimization steps.

The gradient method, for example, is obtained taking $\delta\mathcal{F}(r_i) = \varrho L(r_i)$, $\varrho > 0$, so to let $\delta\mathcal{L} > 0$ in the discretization accuracy. For the applications, however, we used the conjugate gradient method.

As already mentioned, the formulation proposed in this paper allows an easy treatment of the flow constraints. When optimizing the fan stage for thrust, it is necessary to keep constant the work done by unit volume by the rotor, that is

$$\int_{\Omega_b} F^\theta \omega r d\Omega = constant \tag{54}$$

where ω is the angular speed. The increments $\delta\mathcal{F}(r_i)$ are constrained to lay on the manifold determined by eq. (54). Discretizing and linearizing such equation, we obtain an hyperplane onto which the gradient can be projected in order to satisfy the constraint. This procedure is much less expensive and complicated than solving an additional partial differential equation (PDE) for the constraint as it would be necessary for usual optimization methods. Clearly the trade-off should be critically evaluated in relation to eventual geometric constraint, which in our method would be treated by an additional PDE.

The design variables for this test case, being the grid 60×24, are 24 for the stator and 24 for the rotor; $\omega = 1.58$. The constraint on the total work done by the rotor allows very small variations of the forces distribution on the rotor itself. This is seen in the gradient components relative to the rotor that are two order of magnitude smaller compared to those of the stator. Indeed in a different test case relative to a single rotor and not shown here, we found that for a gradient residual decreasing of two orders of magnitude, the thrust gain is very limited.

In fig.6 the gradient residual and the thrust are plotted against the optimization step. The gradient decreases of more than two orders of magnitude and the thrust increases about of 100%.

14

The initial and the optimal stage are in figs (4–5); the first blade from left is the rotor, the second is the stator. The flow at the entrance is axial ($\epsilon = 0$).

In the initial configuration, the stator is not exerting any force to the flow, that is, it does not exists at all. In figure 4 is represented the border of a free stream-surface. After the optimization process an optimal force distribution for the stator is found, which increases the thrust by recovering kinetic energy from the flow issuing from the rotor.

6 CONCLUSIONS

In this work we propose and derive an hybrid method for aerodynamic design, and apply it to turbomachinery design. It takes advantage of the inverse solution of the equations to determine optimal flows. As opposed to shape design optimization (SDO), this methodology could be named flow design optimization (FDO). The relative advantages of using SDO or FDO must be evaluated case by case considering the number of flow constraints relative to geometric constraints. For aerodynamic components where the flow quality is vital, we advocate the preferential use of FDO.

ACKNOWLEDGMENTS

REFERENCES

[1] A. Iollo, M. D. Salas, Contribution to the optimal shape design of 2D internal flows with embedded shocks, JCP 125, 124-134 (1996).

[2] L. Zannetti, Time dependent method to solve the inverse problem for internal flows, AIAA J. , 18, 754–758, (1980).

[3] L. Zannetti, F. Larocca, Inverse Methods for 3D Internal Flows, AGARD-R-780, 1990.

[4] M. Pandolfi, 'A contribution to the numerical prediction of unsteady flows', AIAA J. 22, pp. 602–610, (1984).

[5] A. Harten, B. Engquist, S. Osher, Uniformly High Order Accurate Essentially Non-oscillatory Schemes, III, JCP 71, 231-303 (1987).

[6] R. Fletcher, Practical methods of Optimization,John Wiley & Sons, (1980)

[7] M.Ferlauto, A.Iollo, L. Zannetti, Coupling of Optimization and Inverse Problem for Aerodynamic Shape Design, AIAA paper 2000-0668, 1999

[8] J.M. Lighthill, A new method of two-dimensional aerodynamic design, Aeronaut. Res. Counc. Repts. and Mem. 2112, 1945.

[9] O. Pironneau, On optimum design in fluid mechanics, JFM 59, 117-128, 1972.

[10] A. Jameson, Aerodynamic design via control theory, ICASE Rep. 88-64, 1988.

[11] R.F. van den Dam, J.A. van Egmond, J.W. Sloof, Optimization of target pressure distributions, AGARD-R-780, 1990.

[12] C. Bena, F. Larocca, L. Zannetti, Design of multistage axial flow turbines and compressors, IMech-E 3rd European Conference on Turbomachinery Proceedings, 635-644, London, 1999.